Journal of Nuclear Materials 389 (2009) 57–61

Contents lists available at ScienceDirect

Journal of Nuclear Materials

journal homepage: www.elsevier.com/locate/jnucmat

$NaTaO_3$ composite ceramics – A new thermoelectric material for energy generation

Wilfried Wunderlich

Tokai University, Graduate School of Engineering, Material Science Department, 259-1292 Hiratsuka-shi, Kitakaname 1117, Japan

A B S T R A C T

Increasing energy demand requires the energy harvesting of any dispersed energy in combustion machines, nuclear, geothermal, photovoltaic or solar-thermal devices by thermoelectric materials. $NaTaO_3$ composite material is suggested in this paper for the first time as such material with reasonable high figure-of-merit in the temperature range from 750 to 1273 K. While pure $NaTaO_3$ with perovskite crystal structure is an insulator, ceramic $NaTaO_3$–Fe_2O_3 (n-type) and $NaTaO_3$–Ag (p-type) composites in mixtures around 30 mol.% are semiconductors with Seebeck coefficients of −250 and 70 mV/K as measured in a self-built device even under closed circuit condtions. The electric conductivity for the n-type material increases from 0.02 mS/m at 773 K to 200 mS/m at 1273 K leading to a power factor of $ZT > 4.5 * 10^{-6}$ at 900 K and $\Delta T = 500$ K. This material was found by *ab initio* calculations using the VASP program. The reason for the high Seebeck coefficient is the large effective mass of $NaTaO_3$ $m^*/m_0 = 12$, the main factor determining the thermoelectric performance. It is also confirmed, that Fe atoms as dopants enter the Ta-site of $NaTaO_3$, up to 8 at.%, and reduces the bandgap.

1. Introduction

For solving the future problem energy supply with fewer burdens to the environment, thermoelectric materials might be the solution, if the efficiency can be increased sufficiently. Especially for high temperature applications, like utilizing the temperature gradient of exhaust fumes in fossil fuel or nuclear power stations, bulk ceramic materials are most appropriate due to their stability. Also a combination with solar heat or photovoltaic cells is useful, because a remarkable temperature differences between solar exposed side and not-exposed side occurs. Calculations showed that especially the waste heat in automobiles, furnaces or power stations can be reused and the total support of thermo-electrics as new energy source may even reach 5% in the next decade, when materials with high efficiency are discovered.

The pervoskite based material Nb-doped $SrTiO_3$ is known as effective thermoelectric conversion material with a $ZT = 0.1$ at 1273 K [1], where $ZT = S^2\ T\ \sigma/\kappa$ is the figure of merit and S the Seebeck coefficient, σ the electric conductivity and k the thermal conductivity. The key parameter for achieving a high Seebeck coefficient and thermoelectric power factor is a large effective electron mass m^* [2–4], which includes all the crystal field effects on traveling electrons. Calculations and experiments showed that the effective mass of $SrTiO_3$ ($m^*/m_0 = 4.8$) can be increased by Nb-doping and oxygen deficit to $m^*/m_0 = 7.2$, while La-doping decreases the effective mass [3]. In nano-layers [5] much larger Seebeck coefficients can be achieved due to the confinement of the two-dimensional electron gas. $KTaO_3$ and $NaTaO_3$ have effective masses of 7.6 and 5.7 [3] and with doping 12, larger than pure $SrTiO_3$. Among different doping elements, Fe was found as suitable n-type doping element for $NaTaO_3$ [6], which is also known for its high photo catalytic performance [7]. The idea to choose Ag as p-type candidate came from the opposite coupling behavior of Fe and Ag in magnetic multilayer systems [8,9], and such studies finally led to the Noble-prize for giant magneto resistance [10].

In this paper at first *ab initio* calculations on Fe- and Ag-doped $NaTaO_3$ are presented. In the next chapter, experimental results microstructure characterization, Seebeck voltage and resistivity measurements are explained and finally further possible improvements are discussed.

2. Calculation method and results

It is well accepted that a large effective mass is required for a large Seebeck coefficient in ceramics. *Ab initio* electronic bandstructure calculations were performed using VASP software [11] in the LDA-GGA approximation with a cut-off energy $E = -280$ eV, $U = 0$ V and sufficient number of k-points. The DOS is convoluted with a Gaussian distribution with a FWHM of 0.2 eV, to approximate the broadening at room temperature. The relevant symmetry points in reciprocal space were chosen according to the standard notifications of the perovskite space group *Pm-3 m*. The path in reciprocal space was focused on the three directions near the Γ-point, because in other directions the bands are strongly curved and not close to the bandgap. The supercell used in these

E-mail address: wi-wunder@rocketmail.com

0022-3115/$ - see front matter © 2009 Elsevier B.V. All rights reserved.
doi:10.1016/j.jnucmat.2009.01.007

calculations is a $2 \times 2 \times 2$ extension of the unit cell, allowing calculations of minimal doping concentration steps of 0.125 = 1/8 for *A*- or *B*-side or 1/24 for O. Energy-versus-volume ($E(V)$) calculations confirmed that the usual lattice constants of 0.3968 nm for $NaTaO_3$ are maintained unchanged, when the doping elements considered in this study, Fe and Ag, enter either *A*- or *B*-side, but the energy lowers only when the doping element enters the *B*-(= Ta)-side (about 0.1 eV/atom).

The effective band masses m_{Bi} were estimated by the one-band-approximation from the curvature of each band i at the Γ point j namely the conduction band minimum (CBM) or valence band maximum (VBM) by fitting this parabolic curve to the bands (1) and the averages over j, namely heavy (h) and light (l) electrons from the same band i were calculated from this formula [3]:

$$\frac{1}{m_{B,i,j}} = \frac{2}{\hbar^2} \cdot \frac{d^2 E_{i,j}}{dk_{i,j}^2}, \tag{1}$$

$$m_{B,i} = (m_{B,i,h}^{3/2} + m_{B,i,l}^{3/2})^{2/3}, \tag{2}$$

with Planck's constant $\hbar$. In pure perovskites the CBM and VBM lie at the Γ-point, so that this averaging in the one-band approximation is valid and the bandstructure masses according to Ref. [2] leads to good agreement with experimental determined effective masses m^* [3]. The nearly-free-electron-approximation can be extended even to the heavily doped semiconductors, where the chemical potential is shifted: As the n-doping increases the valence of the *B*-side, charge neutrality principle requires that the number of oxygen atoms needs to be reduce. We assume here the same mechanism as in Nb-doped $SrTiO_3$, namely that the oxygen vacancies introduces donor states about 300 meV below the CBM and lead to the increased conductivity of the material. Indeed doped $NaTaO_3$-specimens turn their white color into black color when sintered. The value of 300 meV has been confirmed by *ab initio* calculations on $SrTiO_{2.88}$ [3]. For p-doped material we assume that the same happens vice-a-versa, namely that acceptor states are introduced above the VBM, presumably caused by metal ion vacancies.

The calculated bandstructure of Fe-doped $NaTaO_3$ is shown in Fig. 1(a), that of Ag-doped $NaTaO_3$ in Fig 1(b). In the case of n-doping the Ta-$2e_g$ bands have lowered their energy and the bandgap becomes so small (~1 eV), that excitation due to phonons become possible. For p-doping the Ta-$2e_g$ are shifted towards the VB, so that an indirect bandgap with similar width occurs. Compared to pure and Nb-doped $SrTiO_3$ ($m^*/m_0 = 4.8$ and 8), pure $NaTaO_3$ ($m^*/m_0 = 8$) the effective electron mass increases further ($m^*/m_0 = 12$) as can be seen on the flat bands over the entire region $\Gamma - \Delta - X$. In undoped $NaTaO_3$ the hole mass is also large ($m^*/m_0 = 8$). The mass of Ag-doped $NaTaO_3$ (Fig. 1(b)) is smaller due to the indirect bands at Z and Λ-points, but the large effective mass of the VBM in undoped regions ($m^*/m_0 > 20$) seems to have also an large influence on the effective mass measured in experiments. The following experimental results support these considerations.

3. Experimental method

$NaTaO_3$ composite ceramics were produced by mixing well-defined weight ratios of fine powders of $NaTaO_3$ (Fine Chemicals Ltd.) and each of the pure metals Ag and Fe, in different concentration ratios in a mortar for more than 10 min. The specimens were pressed with 100 MPa as pellets 10 mm in diameter and 3 mm height and sintered in air first at 1273 K for 5 h, than several times at the same temperature with slow heating and cooling rates (50 K/h). During sintering the white color of $NaTaO_3$ specimens turns into dark color with Fe- and grey with Ag-additions. Between each annealing step the specimens were characterized by SEM (Hitachi 3200-N) at 30 kV equipped with EDS (Noran) and electric resistivity measurements (Sanwa PC510).

The Seebeck voltage was measured in a self-built device (Fig. 2), where the pellet-shaped specimen lies with one end on a $15 \times 15 \times 2$ mm sized ceramics heater (Sakaguchi MS-1000), which can be heated up to 1273 K. The other end lies on a $30 \times 10 \times 10$ mm sized copper block, which acts as heat sink. 1 mm thick Ni-wires are lying below and above the specimen, so that the Seebeck voltage U_S can be measured with attached voltmeters U1 below (and U2 above) the specimen (Fig. 2(a) and (b)). Thermocouples are attached to the specimen at the hot and the cold side and all data were recorded in situ in an attached computer. When comparing such measured data with literature data on similar specimens (CoTiSb, Fe), in general somewhat higher values for the Seebeck voltages are obtained, because usually small temperature gradients of a few K are used, while here a steep gradient up to 700 K is present. As an option, the wires below the

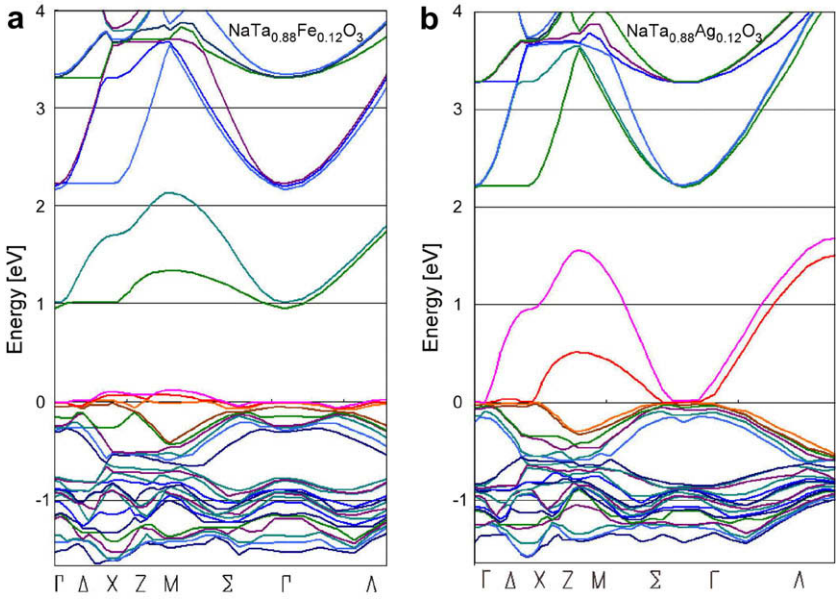

Fig. 1. Electronic bandstructure of (a) $NaTa_{0.88}Fe_{0.12}O_3$ and (b) $NaTa_{0.88}Ag_{0.12}O_3$, as calculated by $2 \times 2 \times 2$ extended supercells.

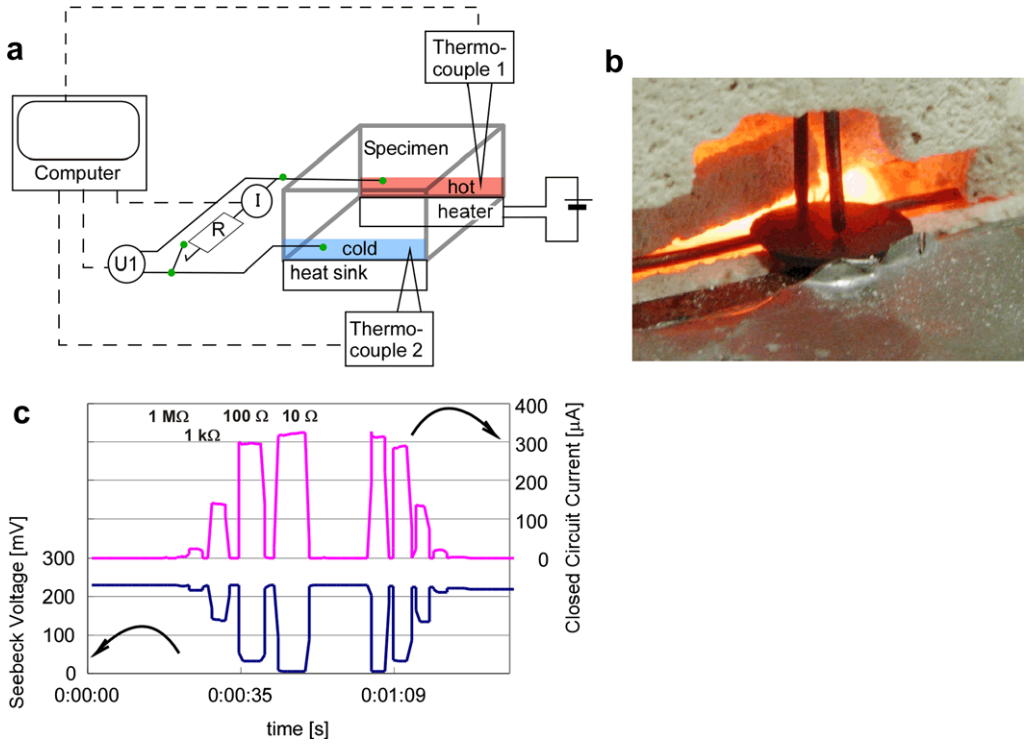

Fig. 2. Device to measure the temperature dependence of the Seebeck voltage below and above the specimen (U1, A, R are voltmeters, ampere meter and an optional resistance in the closed circuit condition, when the switch near R is closed). The broad line shows the specimen lying on one end on the heater, on the other end on the heat sink; hatched lines show the input data connections to the computer. (a) Schematic drawing, (b) specimen during measurement and (c) Seebeck Voltage U_S and electric current as function of time, when the electric circuit between hot and cold side is closed by using different values of resistances R.

specimen were connected with resistances of $R = 10\ \Omega$, $100\ \Omega$, $1\ k\Omega$, or $1\ M\Omega$ in a closed circuit condition and electric current was also measured and recorded. As shown in Fig. 3 for the $NaTaO_3$–30 mol.% Fe_2O_3 specimen, as soon as the circuit is closed the voltage drops down and the current increases according to the amount of load with a delay time of a few ms. The detection limits are about $U_S = 1$ mV and $I = 0.8$ μA. By putting the specimen completely above the ceramics heater, the temperature dependence of the electric resistivity was measured with the same device.

4. Experimental results

XRD measurements confirmed that after sintering the $NaTaO_3$–Fe mixtures changed to $NaTaO_3$–30 mol.% Fe_2O_3 composites (details are reported elsewhere [6]) and the amount of weight increase corresponds to the gain of oxygen. The microstructure consists of 3 μm sized Fe_2O_3 dark particles embedded in the grey $NaTaO_3$ matrix (Fig. 3(a)) as confirmed by SEM and EDX. The volume fraction of particles of 30% corresponds well to the originally weighted-in quantity. The amount of pores remaining from insufficient compaction is about 10%. In the case of Ag about 30% dark metallic particles with a diameter of about 5 μm are observed. SEM-EDX confirmed that in n-type specimens about 8 at.% Fe and in p-type specimens about 2% Ag gets dissolved into the $NaTaO_3$ matrix after sintering at 1273 K 5 h.

The measurements of the Seebeck voltage U_{See} are shown in Fig. 4, for the specimens $NaTaO_3$–Fe (n-type) and $NaTaO_3$–Ag (p-type) both with 30 mol.%. The Seebeck coefficient as deduced from the slope $S = dU_S/dT$ in Fig. 4 for both specimens is almost

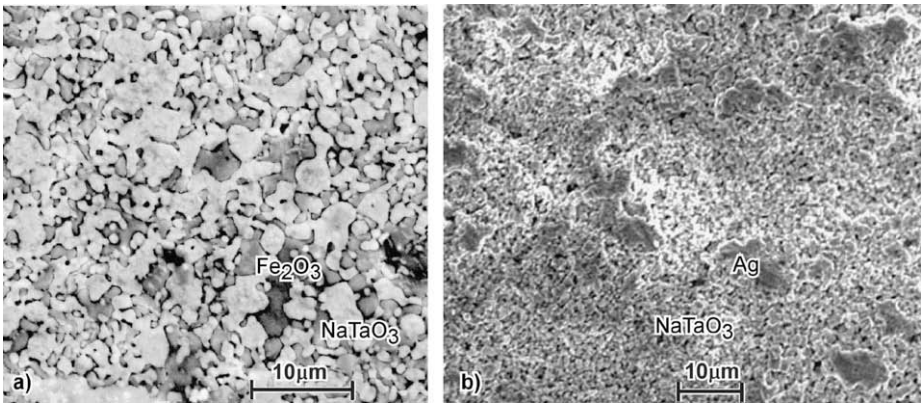

Fig. 3. SEM micrograph of the specimen: (a) $NaTaO_3$ with 30 mol.% Fe_2O_3 and (b) $NaTaO_3$ with 30 mol.% Ag.

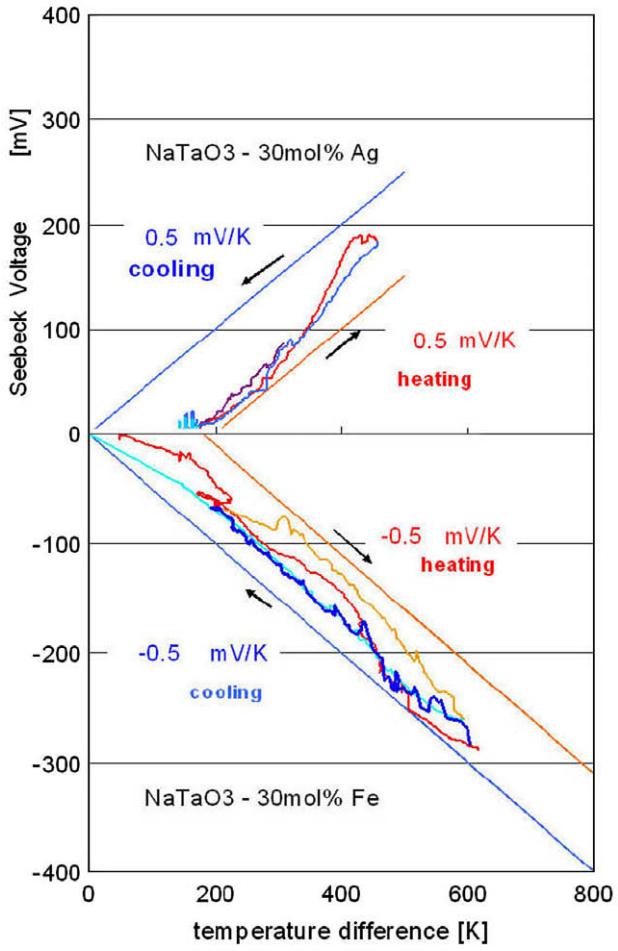

Fig. 4. Seebeck Voltage of $NaTaO_3$–30 mol.% Ag (p-type) and $NaTaO_3$–30 mol.% Fe_2O_3 (n-type) as a function of the temperature difference ΔT between hot and cold end of the specimen. The measuring temperature is approximately $T = \Delta T + 380$ K, where 380 K is the upper temperature at the heat sink. The straight lines represent the data fitting as assuming a linear slope $S = dU_S/dT$ with a Seebeck coefficient of $S = 0.5$ mV/K.

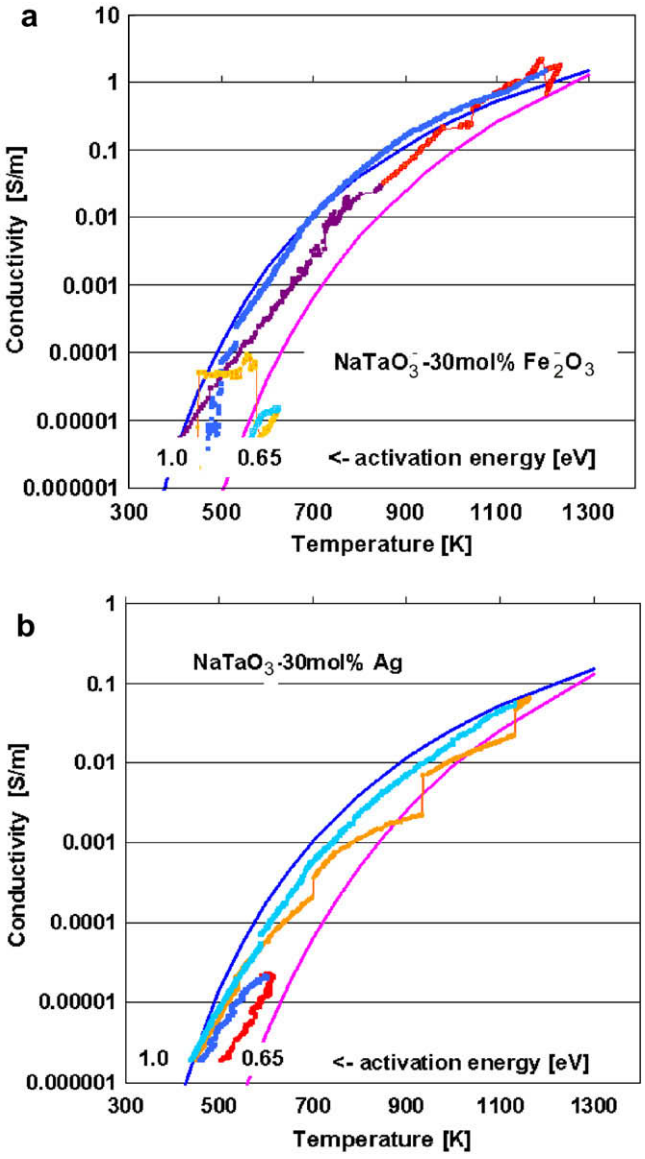

Fig. 5. Temperature dependence of the conductivity σ for (a) $NaTaO_3$–30 mol.%-Fe_2O_3 (n-type), (b) $NaTaO_3$–30 mol.% Ag (p-type). The lines are fits according to $\sigma = N_0 \exp(-E_0/2kT)\,|e|\,\mu_e$. with E_0 activation energy.

the same ±0.5 mV/K, in both, heating as cooling cycles up to the temperature limit of the device at 1273 K, which generates a temperature difference of 600 K. Such values of S were obtained for specimens with compositions $NaTaO_3$–x mol.% Fe with $x = 30$, 50 and 60, while specimens with $x = 20$ and 70 showed remarkably smaller values [6]. The Seebeck voltage increases during the first three sintering cycles (1273 K 5 h), and reached this saturation value, which was confirmed to be stable even after eight sintering cycles. In the case of Ag-doped $NaTaO_3$, the value also increases, however, after the fourth sintering cycle the Seebeck voltage drops to less than 30 mV and the color turns into white again, indicating a structural instability of the $NaTaO_3$–Ag compound probably due to silver evaporation. The temperature dependence of the electric resistivity is shown in Fig. 5 for both, n- and p-type specimens, with 30 mol.%, which was found as the optimum concentration for low resistivity. According to the thermal activation of the carriers, an activation energy in the order of the band gap (1 eV) can be estimated by fitting the data as shown in Fig. 5 by the formula $\sigma = N_0 \exp(-E_0/2kT)\,|e|\,\mu_e$. with E_0 activation energy.

For power generation the performance under closed circuit conditions is important. Fig. 6 shows the measured current when different electric resistances as load are connected. In both n-, and p-type doped specimens the ratio of 30 mol.% seems to be an optimum between large Seebeck coefficient and low resistivity. $NaTaO_3$–x mol.% Fe_2O_3-composite the specimen with $x = 30$ shows the highest current (300 μA) in the closed circuit, while in the case of $NaTaO_3$–Ag compounds the current was close to the detection limit of 0.3 μA and the microstructure needs to be optimized for improving both, Seebeck voltage as well as resistivity.

5. Discussion

The doping of $NaTaO_3$ by Fe or Ag turns the insulator $NaTaO_3$ into n- or p-type semiconductors, as confirmed by bandstructure calculations as well as by experiments. Whether the difference in effective masses ($m^*/m_0 = 12$ for Fe-, $m^*/m_0 = 8$ for Ag-doping) is responsible for the large Seebeck voltage of Fe-doped compared to the smaller value for Ag-doped specimens, is yet unclear, it could also be the different solid solution concentration in $NaTa_{1-z}Me_zO_3$ $z = 0.08$ for Fe or $z = 0.02$ Ag as measured, or the lower conductivity of $NaTaO_3$–Ag (Fig. 5). The activation energy for the charge carriers as can be concluded from the temperature dependence of the resistivity agrees well to the bandgap in the electronic

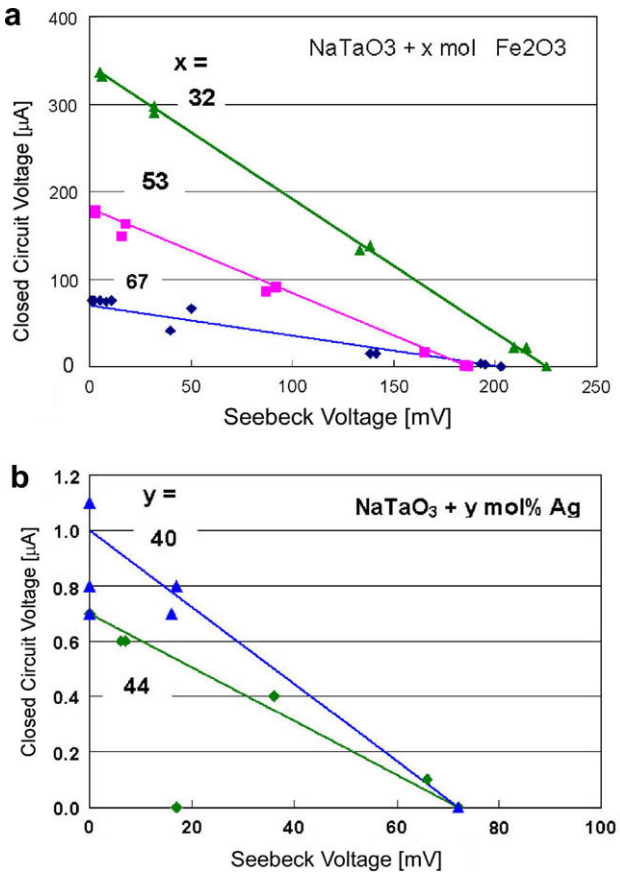

Fig. 6. Under closed circuit conditions, the Seebeck voltage decreases linearly with the electric current; (a) $NaTaO_3$–x mol.% Fe_2O_3 (n-type) with $x = 30$, 50 and 70, (b) $NaTaO_3$–y mol.% Ag, $y = 30$ and 40. The electric current strongly depends on the amount of second phase, while the Seebeck Voltage not.

band structure calculations (1 eV). The carrier concentration is still so small, that only above 750 K ($\Delta T > 477$ K) the conductivity is high enough, to achieve a remarkable Seebeck coefficient. An increase of the solid solution concentration in $NaTa_{1-z}Me_zO_3$ beyond $z = 0.08$ (Fe) or 0.02 (Ag) would help, but the attempt to achieve this by an increased amount of second phase x or y due to a steeper diffusion gradient, had in fact the opposite effect that the conductivity of the composite dropped down when x or y became larger than 30 mol%. On the other hand, the second phase is obviously necessary, since specimens with x or $y < 20\%$ are almost insulators even at high temperatures. While $NaTaO_3$–Fe_2O_3 is a stable composite, the metallic Ag in the p-type composite with its low melting point seems to decompose or turns into an insulating oxide. $NaTaO_3$–30 mol% Fe_2O_3 specimens showed a Seebeck coefficient of -0.5 mV/K, or $U_S = -250$ mV at $T = 800$ K ($\Delta T = 500$ K) and was confirmed even under load. Together with the conductivity of $\sigma = 1/\rho > 1/(5\ \text{Ohm m})$ (Fig. 5(a)), the following lower limit for the figure of merit can be deduced, when for the thermal conductivity the worst case of a high value of 10 W/(mK) is assumed [1], while usual such ceramics lie in the range of 5 W/(mK). This leads to:

$$Z = \frac{S^2 \cdot \sigma}{\kappa} > \frac{(0.50\,\text{mV/K})^2 \cdot 0.2\,\text{S/m}}{10\,\text{W} \cdot m^{-1} \cdot \text{K}^{-1}} = 5.0 \times 10^{-9}\,\text{K}^{-1}, \quad ZT_{900\,\text{K}} > 4.5 \times 10^{-6} \tag{3}$$

which is still less than values of present n-doped thermoelectrics like Nb–$SrTiO_3$ [1] or SiGe [2] in this high temperature range. Advanced ceramic processing like spark plasma sintering, hot-isostatic pressing, precursor derived Ag–nano-ceramic-composites [12] or even n-type/insulator-nano-layers as in Nb–$SrTiO_3$ [5] would be able to improve the microstructure and hence increase both, Seebeck coefficient as well as conductivity. Furthermore, the alloy composition has to be optimized as in this quaternary compound many kinds of vacancies or other defects might occur.

6. Conclusion

$NaTaO_3$ ceramic composites are suggested as a new thermoelectric material either for power generation or as Peltier coolers suitable for applications in an upper range of application temperatures (750–1300 K). Bandstructure calculations suggested these n- and p-type materials due to their large values of effective masses for Fe- or Ag-doping. Although the microstructure needs to be optimized, promising ZT values of $ZT > 4.5 * 10^{-6}$ at 900 K are estimated and Seebeck voltages of -250 mV (n-type) and 70 mV (p-type) have been measured. These values were measured on $NaTaO_3$–x mol.% Fe_2O_3 and Ag in the range of $x = 30$–60, but under load only composites with $x = 30$ shows large currents.

Acknowledgments

The author acknowledges help from Sadao Yoshimura, Susumu Soga and Yoshiyuki Kondo.

References

[1] S. Ohta, T. Nomura, H. Ohta, K. Koumoto, Appl. Phys. Lett. 87 (2005) 092108.
[2] A. Bulusu, D.G. Walker, Superlattice Microstr. 44 (1) (2008) 1.
[3] W. Wunderlich, H. Ohta, K. Koumoto, arxiv:/arXiv/cond-mat0510013.
[4] W. Wunderlich, K. Koumoto, Int. J. Mater. Res. 97 (5) (2006) 657.
[5] Kyu Hyoung Lee, Yoriko Muna, Hiromichi Ohta, Kunihito Koumoto, Appl. Phys. Exp. 1 (2008) 015007.
[6] Wilfried Wunderlich, Susumu Soga, Mater. Trans., in press.
[7] H. Kato, A. Kudo, Chem. Phys. Lett. 295 (5&6) (1998) 487.
[8] A.T. Costa Jr., J. d'Albuquerque e Castro, R.B. Muniz, Phys. Rev. B 56 (1) (1997) 13697.
[9] M. Sternik, K. Parlinski, Phys. Rev. B 75 212406 (2007).
[10] P. Grünberg, J. Phys.: Condens. Matter. 13 (2001) 7691.
[11] G. Kresse, J. Hafner, Phys. Rev. B 49 (1994) 14251.
[12] Aji A. Anappara, S.K. Gosh, P.R.S. Warrier, K.G.K. Warrier, W. Wunderlich, Acta Mater. 51 (2003) 3511.